OPTIMUM DESIGN OF A TOROIDAL PRESSURE VESSEL OF COMPOSITE MATERIAL FOR GAS (CNG) POWERED VEHICLES

Darwin Patiño Pérez[1,2,3], Alfonso Corz Rodríguez[1]

[1]Universidad de Cádiz. Escuela Politécnica Superior de Algeciras, Grupo de I+D, Materiales Compuestos. Avda. Ramon de Puyol, s/n – 11202 Algeciras (España). darwin.patinoperez@alum.uca.es , alfonso.corz@uca.es

[2]Universidad de Guayaquil. Facultad de Ciencias Matemáticas y Física. Carrera de Ing. en Sistemas Computacionales, Cdla. Salvador Allende, Av. Delta y Av. Kennedy – Guayaquil (Ecuador)

[3]West Virginia University. College of Engineering and Mineral Resources, Department of Mechanical and Aerospace Engineering, PO Box 6106,395 Evansdale Drive - Morgantown, West Virginia 26506-6106 (EE.UU)

Received: 21/Jan/2019 - Reviewed: 14/Feb/2019 - Accepted: 21/Mar/2019 - DOI: http://dx.doi.org/10.6036/9096

ABSTRACT:

In the present work to design is made, using numerical simulations, with the finite element method (FEM) to linear elastic analysis will be performed for the optimal design of a toroidal pressure vessel resistant, lightweight and capable of storing compressed natural gas (CNG) for vehicles.

For the design the material AS/3501 (carbon fiber and epoxy matrix) is used, since there are studies that indicate that, with this type of material, high resistances and better performance have been obtained than with metallic materials.

The analysis will determine the influence exerted by the angular orientation of the layers in the strength of the laminate, in addition to the variation of stress, strain and displacement that occurs in the toroid, when it is subjected to pressure.

The optimization of the volume of the material, will be made with the metaheuristic algorithm called Particles Swarm Optimization (PSO), which will use Threads in Java for the execution of the scripts developed in ANSYS for the analysis of the FEM and with which will be reduced computing times improving to the optimizer.

Key Words: pressure vessel, toroidal shape, finite elements, numerical simulations, optimization, threads.

RESUMEN:

In the present work to design is made, using numerical simulations, with the finite element method (FEM) to linear elastic analysis will be performed for the optimal design of a toroidal pressure vessel resistant, lightweight and capable of storing compressed natural gas (CNG) for vehicles.

For the design the material AS/3501 (carbon fiber and epoxy matrix) is used, since there are studies th
at indicate that, with this type of material, high resistances and better performance have been obtained than with metallic materials.

The analysis will determine the influence exerted by the angular orientation of the layers in the strength of the laminate, in addition to the variation of stress, strain and displacement that occurs in the toroid, when it is subjected to pressure.

The optimization of the volume of the material, will be made with the metaheuristic algorithm called Particles Swarm Optimization (PSO), which will use Threads in Java for the execution of the scripts developed in ANSYS for the analysis of the FEM and with which will be reduced computing times improving to the optimizer.

Keywords: pressure vessel, toroidal shape, finite elements, numerical simulation, optimization, threads.

1.- INTRODUCTION

One of the challenges facing in the energy field, is the transformation of the compressed natural gas (CNG) in energy, its low cost and reduction of environmental pollution, are factors for use as fuel in the automotive industry[1], requiring resistant containers for storage. One of the main barriers in the design of containers is the adaptability and the ability to store enough CNG to generate the same or greater amount of energy generated by the diesel or gasoline[2].

They are generally used metal cylinders for the storage of CNG, weighing between 110.23lb(50Kg) and 427.7lb(194Kg), and can store between 80L and 200L of gas, enduring a pressure of approximately 2.9001ksi(200bar)[3], but there are studies that indicate that the containers are suitable for the toroidal gas storage[4], so that have been used in the aviation industry, shipbuilding and automotive industries in different types of vehicles; initially were made of isotropic material such as steel , but as new technologies have been developed from composite materials have been redesigned these containers with good results.[5]. The use of composites materials in toroidal pressure vessels offers many advantages over conventional materials and have a lighter weight and a great capacity to adapt to the requirements of design; the rigidity, resistance and weight, are some properties of the *composites*, that are

not found in a single material, because they are derived from a combination of the properties of the materials that make up[6].

The carbon fiber[7] It has a crystalline microscopic structure composed of carbon atoms, for their manufacture[8] Take thousands of carbon filaments that are joined together to form a thread, which usually has a diameter between 5 or 10 microns. The fiber along with the resin matrix, forms a composite material that stands out among others for their good properties. The matrix has the function to maintain the shape of the composite structure, maintain aligned fibers and act as a means of transfer of tension and at the same time as an element of protection of the fibers. The carbon-epoxy composite material, has an acceptable cost, so its use allows to obtain materials of low weight, high-strength and high stiffness, and are widely used in the aviation industry as in the Boeing B787[9] or in the A350 XWB Airbus-[10] and in the automotive industry[11].

Obtain solutions, business travel and tensions in a toroid, are more difficult to obtain than in other axisymmetric shells of revolution, due to the peculiarities of the equations in different places in the toroid and mainly in its crest (Fig.1b); several elastic solutions, for orthotropic toroid subjected to internal pressure are available in the literature. [12],[13] and optimizations have been considered in the design manufactured by wrapping toroid with fiber[14],[15],[16]. Using optimization techniques to troubleshoot complex problems, so that with classical techniques is the optimal solution and it is demonstrated that it is the best way to ensure local minima, so sometimes have a low performance. On the other hand, are approximate techniques that avoid, as far as possible, the problem of local minima, but the optimal solution is only approximate.

Among the approximate techniques, optimization metaheuristics[17] They are considered a high-level generic strategies. *Particle Swarm Optimization* (PSO) is an algorithm that performs metaheuristic explorations in search spaces of great size, flexibility and adaptability (described by *James Kennedy and Russell C. EBERHART*) was initially created for the modeling of social behaviors that are reflected in the nature, such as the movement of a bank of fish or a flock of birds[18], At the time of a deep search makes it in the space where there is the greatest likelihood of finding what you are looking for[19]; This idea was forwarded to the field of computing as an algorithm for solving problems that arise with many variables, functions and whose objective is to find the optimal solution or a very close to the optimal[20].

In the present work will aim to optimize a toroidal container M5, from the comparative analysis of pressure vessels of toroidal in shape with composite material recorded in[21] , Its geometry is a function of the radius R=14in(355.6mm) and a=6in(152.4mm) and the thickness of the laminate will be t=0.75in (19.05mm). To find the solutions are used numerical simulations with the finite element method (FEM), because they offer high reliability in the values of variables and greater precision in the results; in the model will be carried out variations of the angles of the laminate sheets at each iteration to determine the resistance. Once optimized will analyze the model, and the benefits that are obtained for the storage of CNG in comparison with the cylindrical containers that are currently used.

2. MODEL AND METHODS

2.1.- TOROIDAL MODEL

2.1.1.- Geometry of the toroid.

The toroid circular (Figure 1a) has been formed by turning a cross section (section (straight line) from radio **to** around an axis of rotation(axis) whose radius R is the radius of the toroid (Figure 1b), the thickness **t** usually it is assumed constant for metallic materials but can vary for orthotropic materials[22];

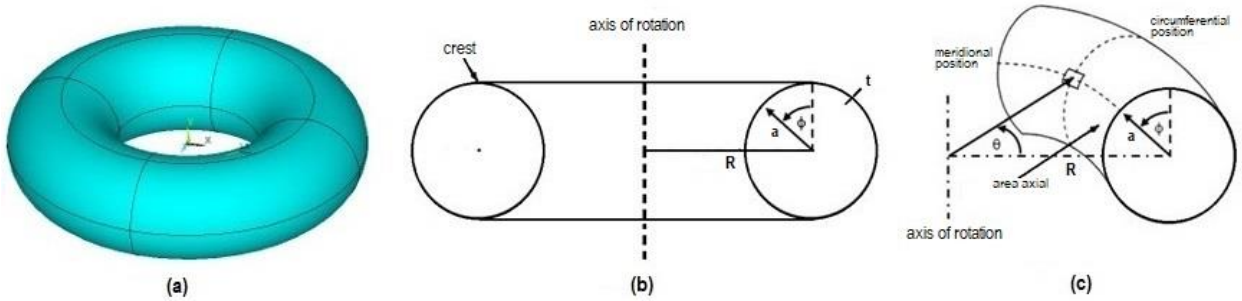

Fig. 1: Geometry of the toroid

The southern direction ϕ for a circular toroid is tangent to the straight section, and the circumferential direction θ continues the circle of revolution for the toroid (Figure 1c). The top half of the toroid is defined on the basis of $-90° < \phi < 90°$, with a crest that occurs in $\phi = 0°$.

Due to its geometry, the toroid winding of fiberboard has a thickness variations natural due to the accumulation of fiber. The volume of the fiber is constant through the toroid; therefore, the thickness of the toroidal shell decreases radially from the axis of revolution due to the increase in the surface of the toroid. The thickness of the *shell* can be defined as a function of the southern coordinate ϕ, and can take as reference the thickness in the crest of the toroid t_c [23].

$$t(\phi) = \frac{R \cdot t_C}{R - a \cdot \sin\phi} \qquad (1)$$

The efforts of membrane into the southern and circumferential directions [23], according to the theory of membranes are:

$$N_\phi = \frac{p.a}{2}\left(1 + \frac{R}{R - a \cdot \sin\phi}\right) \quad \text{y} \quad N_\theta = \frac{p.a}{2} \qquad (2)$$

The tension is considered constant through the thickness of an isotropic material and is related to the effort in the shell (shell) $N = \sigma.t$; the southern effort N_ϕ, decreases as the distance from the axis of revolution increases while the hoop stress N_θ, remains constant through the toroid, so the southern load is dominant within it. The balance of efforts in the *shell* of revolution under internal pressure p is given by:

$$\frac{N_\phi}{R_\phi} + \frac{N_\theta}{a} = p \qquad (3)$$

R_ϕ is the radius of curvature meridional and **a** is the radius of curvature circumferential.

The tensions longitudinal and circumferential joints of the toroid and radio to radio similar cylinder, which has 2 heads of the same radio, hemispherical can determine who is more resistant, so that the longitudinal tension (σ_l) and circumferential (σ_c) both would be[5]:

Tensions in the cylinder

$$\sigma_l = \frac{p.a}{2t} \quad ; \quad \sigma_c = \frac{p.a}{t} \qquad (4)$$

Tensions in the toroid

$$\sigma_l = \sigma_\theta = \frac{p.a}{2.t} \quad ; \quad \sigma_c = \sigma_\phi.C = \frac{p.a}{t}.C \qquad (5)$$

The coefficient C, depends on the larger radius (R) and minor radius (a) of the toroid, in addition to the position ϕ :

$$C = \frac{1}{2}\left(1 + \frac{R}{R - a \cdot \sin\phi}\right) \qquad (6)$$

$$C_{\phi=0} = 1 \;\; ; \phi = 0 \; ; \;\; \sigma_{\phi} = \frac{p.a}{t} \qquad (7a)$$

$$C_{\phi=90} = \frac{1}{2} + \frac{1}{2\left(1-\frac{a}{R}\right)} \qquad (7b)$$

$$C_{\phi=-90} = \frac{1}{2} + \frac{1}{2\left(1+\frac{a}{R}\right)} \qquad (7c)$$

For values of R between 2a and 10a, we have:

$$R = 2a \qquad C_{\phi=90} = \frac{3}{2} \;\; ; \;\; \sigma_{\phi=90} = \frac{p.a}{t}.\frac{3}{2} \qquad (8a)$$

$$R = 2a \qquad C_{\phi=-90} = \frac{5}{6} \;\; ; \sigma_{\phi=-90} = \frac{p.a}{t}.\frac{5}{6} \qquad (8b)$$

$$R = 10a \quad C_{\phi=90} = \frac{19}{18} \;\; ; \;\; \sigma_{\phi=90} = \frac{p.a}{t}.\frac{19}{18} \qquad (8c)$$

$$R = 10a \quad C_{\phi=-90} = \frac{16}{22} \;\; ; \;\; \sigma_{\phi=-90} = \frac{p.a}{t}.\frac{16}{22} \qquad (8d)$$

Therefore, for the toroid as a function of the ratio R/a=2 the tensions will evolve according to the point at which the value of ϕ being considered; in the worst case , there will be a variation between 1.5 and 0.84, which in so far as it increases the ratio r/a, this difference decreases; it was furthermore that for R/a=10 the variation is between 1.05 and 0.72, in both cases this variation goes through 1. With regard to the cylindrical pressure vessel, the maximum strain is for the most unfavorable point and the most unfavorable case is 1.5 times greater, although the average value would be 1.17 times.

The surfaces and volumes are of the same order, so that the advantage you have with the toroidal pressure vessel is your space use to be compact; to be important differences between the tensions generated in two orthogonal directions, it would be ideal to have a material with elastic properties.

The volume of the toroid without including the wall

$$V_t = 2.\pi^2.R.a^2 \qquad (9)$$

To replace ***by a + t*** would include the wall

$$V_{tpi} = 2.\pi^2.R.(a+t)^2 \qquad (10)$$

Since $V_{tpi} > V_t$ **the volume of the wall of the toroid** V_{pt} what determines the difference between EC (10) and EC (9)

$$V_{pt} = V_{tpi} - V_t = 2.\pi^2.R.\left(2.a.t+t^2\right) \qquad (11)$$

The margin of difference between the analytical calculation Ec (11) and the value offered by the FEM would be

$$\text{margen} = 100 \cdot (V_{pt} - V_{MEF}) / V_{pt} \quad (12)$$

2.1.2.- The Laminate.

The criteria of the laminate of the toroid come from the literature the angles of the layers of laminate (Figure 2a), exert a lot of influence when it has to withstand loads in different directions, the resistance and stiffness are generally higher in the direction of the fibers with respect to the transverse direction.

For toroid built with composite materials, the orthotropic constitutive relation can be defined using the theory of rolled products given in[24],[25],[26]

$$\begin{Bmatrix} N \\ M \end{Bmatrix} = \begin{bmatrix} A\,B \\ B\,D \end{bmatrix} \begin{Bmatrix} \varepsilon^{\circ} \\ K \end{Bmatrix} \quad (13)$$

Where **N** is the vector of forces per unit length, **M** is the vector of moments per unit length, **Eo** is the vector of deformations in the midplane, and **K** is the vector of curvatures on the midplane. The laminate is constant being A, B and D matrices of stiffness, where **A** is the matrix of stiffness tv, **B** is the matrix of coupling and **D** is the matrix of stiffness of flexion. These are the basis of the general equation of the classical theory of laminated wood panels, they relate to the forces in the plane and the resulting moments per unit of length, with the deformation and the curvature of the reference plane of the laminate[24],[25]

$$|A| = \sum_{i=1}^{n} \left[\overline{Q}\right]^{i} (z_i - z_{i-1}) \quad (14a)$$

$$|B| = \frac{1}{2} \sum_{i=1}^{n} \left[\overline{Q}\right]^{i} (z_i^2 - z_{i-1}^2) \quad (14b)$$

$$|D| = \frac{1}{3} \sum_{i=1}^{n} \left[\overline{Q}\right]^{i} (z_i^3 - z_{i-1}^3) \quad (14c)$$

For a laminate containing n layers. $\left[\overline{Q}\right]^{i}$ corresponds to the transposed from the matrix of stiffness of the i-th layer laminate and Z_i corresponds to the distance from the plane-middle of the laminate to the edge of the layer i (Figure 2b). These arrays differ from other constituent constants (Young's modulus) due to the fact that they contain geometric information about the laminate that is affected by the conditions of the term Z_i.

The main constants of engineering for a laminate can be determined from the stiffness matrix A in the plane, according to the laminate **a*** is defined by[24].

$$\left\{\varepsilon^{o}\right\} = \left[a^{*}\right]\left\{\overline{\sigma}\right\} \text{ donde } \left[a^{*}\right] = \begin{bmatrix} a_{11}^{*} & a_{12}^{*} & a_{16}^{*} \\ a_{12}^{*} & a_{22}^{*} & a_{26}^{*} \\ a_{16}^{*} & a_{26}^{*} & a_{66}^{*} \end{bmatrix} = t\left[A\right]^{-1} \quad (15)$$

$$\left\{\overline{\sigma}\right\} = \left[Q\right]\left\{\overline{\varepsilon}\right\} \text{ donde } \left\{\overline{\varepsilon}\right\} = \begin{bmatrix} m^2 & n^2 & mn^2 \\ n^2 & m^2 & -mn \\ -2mn & 2mn & m^2 - n^2 \end{bmatrix} \begin{Bmatrix} \varepsilon_1 \\ \varepsilon_2 \\ \varepsilon_{12} \end{Bmatrix} \quad (16)$$

donde $\overline{\sigma}$ Is the vector of the average of the tensions flat, Q Is the matrix of stiffness of the layer, $\overline{\varepsilon}$ Is the deformation of the layer turned on by α_i From the global coordinate system (Figure 2c) in the direction of the fiber, $m = \cos(\alpha_i)$ y $n = \sin(\alpha_i)$ The Ec. (16) directly provides the address of the fiber, the transverse direction and the

tensions of flat court within each layer, which allows a comparison of the states of tension within each layer through the cross-section of the toroid and provides the basis for the optimization process.

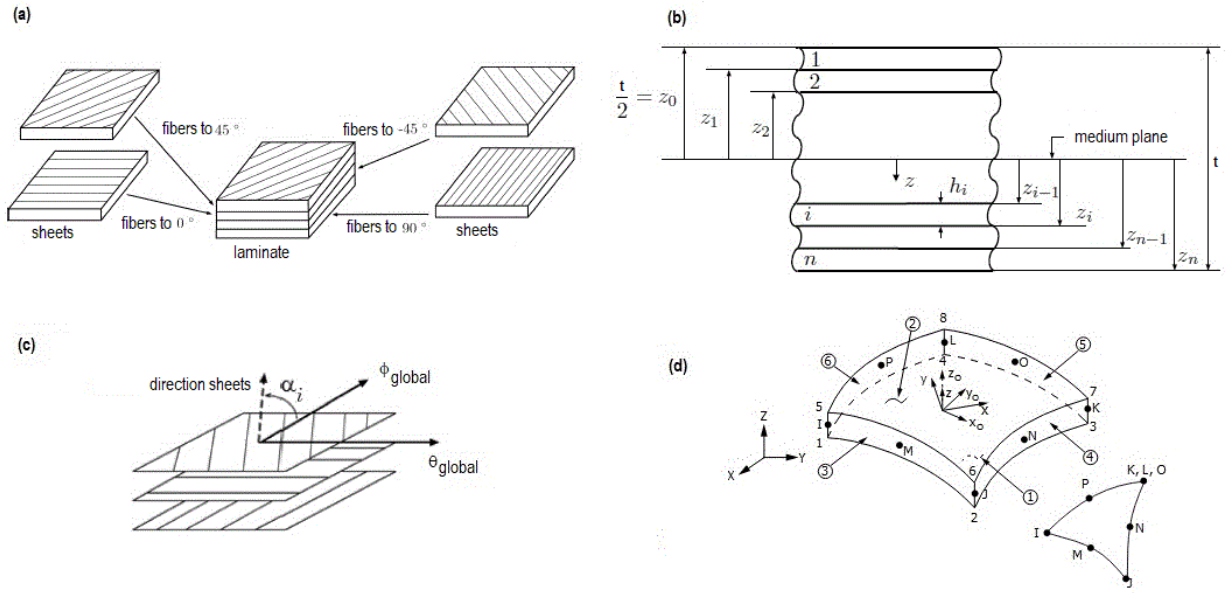

Fig. 2: Laminating and geometry of the shell element281

The properties of the shell element of multiple layers are determined by the theory of laminates, the appropriate element for the analysis of thin-wall structures is the shell281 (Figure 2d), as has 8 quadrilateral nodes with 6 degrees of freedom, in each node: you can give translations in the three axes (x, y, z) and rotations about the three axes, can be used considering the theory of membrane and bending or only the membrane (in this case has 3 degrees of freedom per node and are only translations); this element is suitable for linear elastic analysis by large rotations that may occur and/or large deformations in Non-linear in applications where you can take into account variations in thickness, it can also be used for modeling multi-tier applications, composite shells or sandwich constructions, the precision in the modeling with shell made of composite material is governed by the theory of *Reissner-Mindlin plates* [25].

The mechanical properties of the sheets, are given by the direction of the fibers, and the micromechanics of them allows us to get parameters that mark its mechanical behavior[27]. These materials are characterized the orthotropic elastic constants associated with three mutually perpendicular directions and have an elastic behavior represented by nine independent constants formed by three longitudinal modulus of elasticity (E_1,E_2,E_3), Three modules of rigidity (G_{12},G_{23},G_{13}) And three coefficients of Poisson $(\nu_{12},\nu_{23},\nu_{13})$. In the case of a sheet are reduced to four constants: E_1,E_2,G_{12},ν_{12} ; Being $G_{12}=G_{13}$ And $\nu_{12}=\frac{E_1}{E_2}\nu_{21}$, Where the direction of the fibers is indicated by the subscript 1 and the transverse direction to the fibers with a subscript 2; ν_{12} Is the Poisson's ratio in the direction of the fibers and ν_{21} It is the same coefficient in the transverse direction.

The lamination technique considered in this study, it is called an *Automated Fiber Placement* (AFP) [28], Consists in the automatic application of bands of carbon fiber pre-impregnated with epoxy on the mold of the toroid, the advantage of this technology, is the minimum cut length of layers at the surface of the workpiece, the thickness of the bands will normally be less than 0.315in(8mm), this technique allows that we can work on parts with very complex contours[29].

2.2.- MATERIAL

Unidirectional blades made of composites material AS/3501 formed by carbon fiber(AS) and epoxy resin matrix(3501) are considered for the optimization process, in tests on similar literature the material offers good performance on toroidal pressure vessel under pressure [21].

Property	Value	Unit	Value	Unit	Description
E_1	20.02	Msi	138	GPa	Elasticity module
E_2=E_3	1.30	Msi	8.96	GPa	Elasticity module
G_{12}=G_{13}	1.03	Msi	7.1	GPa	Stiffness module
G_{23}	0.41	Msi	2.82	GPa	Stiffness module
V_{12}=V_{13}	0.30		0.3		Poisson's coefficient
V_{23}	0.59		0.59		Poisson's coefficient
F_{1t}	2.1E+05	Psi	1447	MPa	Longitudinal resistance to traction
F_{1c}	2.1E+05	Psi	1447	MPa	Longitudinal compression resistance
F_{2t}	7.5E+03	Psi	52	MPa	Transverse tensile strength
F_{2c}	2.99E+04	Psi	206	MPa	Transverse tensile strength
F_{3t}	1.0E+06	Psi	1.0E+06	MPa	Resistance (large value that is not calculated)
F_{3c}	1.0E+06	Psi	1.0E+06	MPa	Resistance (large value that is not calculated)
F_4	1.0E+06	Psi	1.0E+06	MPa	Resistance (large value that is not calculated)
F_5	1.0E+06	Psi	1.0E+06	MPa	Resistance (large value that is not calculated)
F_6	1.35E+04	Psi	93	MPa	Longitudinal resistance to shear
C_6	-1		-1		Coefficient, defaults -1
C_4	-1		-1		Coefficient, defaults -1
C5	-1		-1		Coefficient, defaults -1
ρ = 1.6 g/cm³ = 0.0262 Kg/in³					Density of the Composite Material

Table 1: Properties of the Material AS/3501[30].

2.3.- METHOD.

2.3.1.- Numerical Simulation

The numerical simulation is carried out by means of the FEM takes criteria of the literature: [22],[27],[31] that will be used in the script of the ADPL(ANSYS Parametric Desing Language), to perform a linear elastic analysis, the technique of plain to be used will be local and controlled globally in terms of the length of the edge of the element used in the limits of the surface of the same; you will use a plain with 10392 triangular elements, the overall size of the element will be of 0.8in(20.32 mm) with 20784 nodes. The boundary conditions establish restrictions on the shafts Y,Z for nodes 8(R+a,0.0) and 9(-R-a,0.0) and restrictions on the X,Y for nodes 3(0.0,R+a) and 14(0.0, R-) to keep supported the toroid. In the laminate material is used as/3501 whose properties are shown in Table 1, and will be made up of n=12 sheets and each will have a thickness $\frac{t}{n}$, Angular orientation will be [45/-45/0/-45/45/90]s and will be stacked symmetrically. Finally, the model will be subjected to 5000psi(374.44bar) pressure.

2.3.2.- Restriction by the Tsai-Wu Failure Criterion

The criterion of judgment comes from the adjustment curves obtained from experimental tests that are used to predict failures and is represented by the middle of the notation of failure rate, which is used by several packages of finite elements.

$$I_F = \frac{estress}{strength} \quad \text{; is predicted, the failure when; } I_F \geq 1 \qquad (16)$$

The resistance is the inverse of the failure rate

$R = \frac{1}{I_F} = \frac{strength}{stress}$; is predicted, the failure when; $R \leq 1$ (17)

The Tsai-Wu criterion is used to determine the fault that occurs in the first layer of a laminate, using this approach, the failure rate is defined as:

$$I_F = \frac{1}{R} = \left[-\frac{B}{2A} + \sqrt{\left(\frac{B}{2A}\right)^2 + \frac{1}{A}} \right]^{-1} \quad (18)$$

with

$$A = \frac{\sigma_1^2}{F_{1t}F_{1c}} + \frac{\sigma_2^2}{F_{2t}F_{2c}} + \frac{\sigma_3^2}{F_{3t}F_{3c}} + \frac{\sigma_4^2}{F_4^2} + \frac{\sigma_5^2}{F_5^2} + \quad (19)$$

$$C_4 \frac{\sigma_2\sigma_3}{\sqrt{F_{2t}F_{2c}F_{3t}F_{3c}}} + C_5 \frac{\sigma_1\sigma_3}{\sqrt{F_{1t}F_{1c}F_{3t}F_{3c}}} + C_6 \frac{\sigma_1\sigma_2}{\sqrt{F_{1t}F_{1c}F_{2t}F_{2c}}}$$

and

$$B = \left(F_{1t}^{-1} - F_{1c}^{-1}\right)\sigma_1 + \left(F_{2t}^{-1} - F_{2c}^{-1}\right)\sigma_2 + \left(F_{3t}^{-1} - F_{3c}^{-1}\right)\sigma_3 \quad (20)$$

Where C_i , i=4..6, are the coefficients of Tsai-Wu coupling, which by default is -1. That compression strength in EC. (18) and EC. (19) are here positive numbers. The through the thickness strength values F_{3t} and F_{3c} , are rarely available in a literature, so it is a common practice to use the corresponding in-plane transverse values of strength[27] , the intralaminar strength F_5 is commonly assumed to be equal to the in-pane shear strength, so lacking experimental data for the remaining intralaminar strength F_4, it can be estimate as the shear strength of the matrix. The description of the strength and coefficients used in the EC. (18) and EC. (19) are recorded in Table 1.

2.3.3.- Experimental Validation of a Toroidal Model

To perform the validation of the model, have provided the data of a toroid which has been tested experimentally by *Haixiao Hu*[16], Which is formed by a "liner" of titanium with thickness t_o = 0.07874in(2mm) and a laminate of aramid fiber and epoxy matrix, with a thick sheet of 0.01417mm(0.36in); this laminate is formed by 12 sheets. Angular orientation is a function of the angle φ whose value is between 0< ϕ <π, also uses an angle α that serves to guide the winding of the fibers and to determine the thickness tα according to the fiber orientation. After the tests using the FEM model developed by us, we proceeded to contrast the results with the experimental results obtained by *Haixiao Hu*[16], obtaining a pressure limit for linear behavior in the trials of 4351.13Psi(30MPa) and a pressure limit in the case of our numerical model of 4303.2729.67Psi(MPa). Given that the error between the numerical model and experimental is 1.1%, it is accepted as valid the methodology of the FEM model for our successive models of toroidal pressure vessels.

2.3.4.- Optimization

The PSO is a method of metaheuristics, each particle of the initial population, runs through the space solution to a speed V to new positions X according to your own experience P and with the experience provided by the best of their fellow G [18]; It is so that the optimization of composite material based on PSO that include FEM have given good results [32].

In (Fig. 3) the flow of the PSO implemented with JAVA, uses a script to the FEM created in APDL, which will run in *batch mode* from each *thread ;* running to optimize to M5[21].

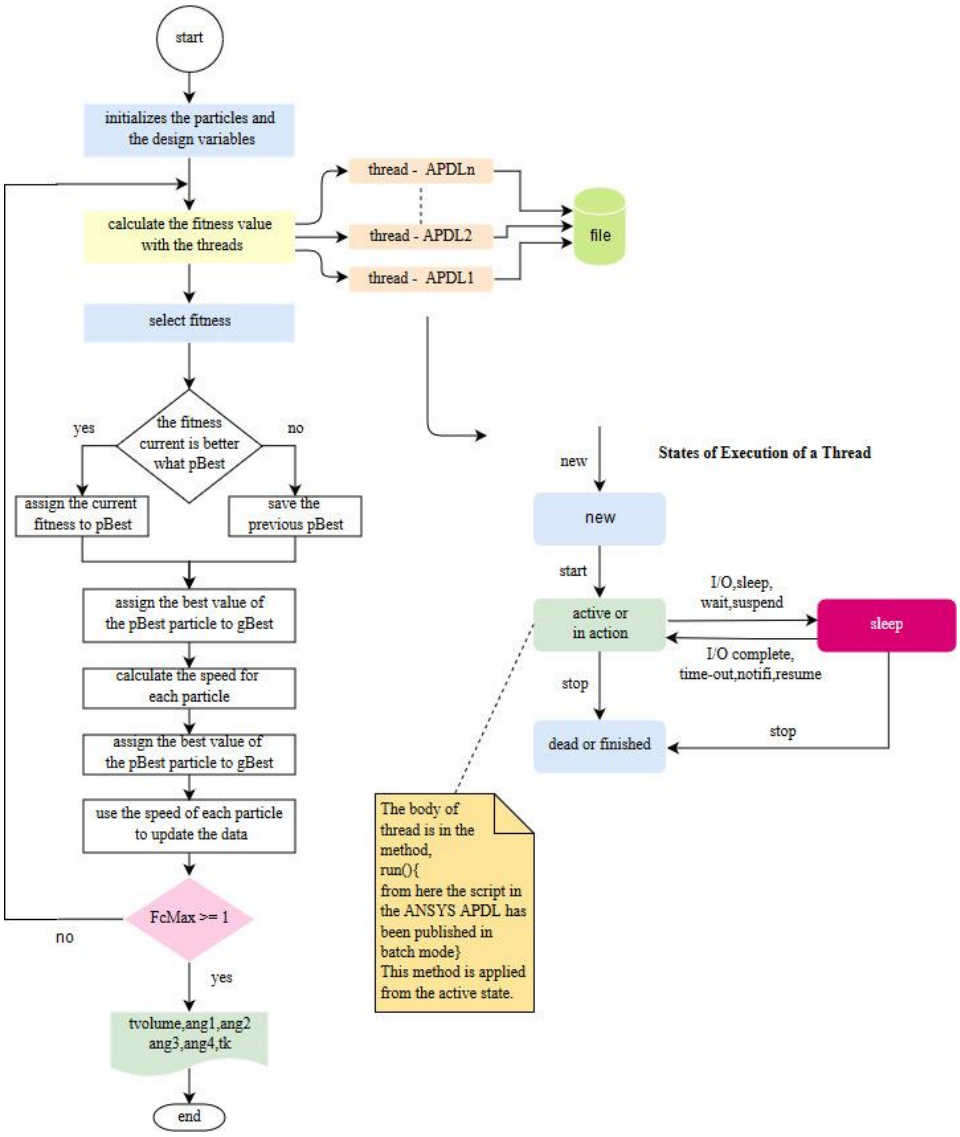

Fig. 3: Particle Swarm Optimization (PSO)

For this algorithm based on criteria of PSO abstracted[33], each particle is associated with an object that has a number of characteristics and properties associated with design variables(DV), state variable(DS) and the objective function(obj) to be minimized; this objective function represents the volume of material (Tvolume) to be optimized, design variables are associated to the angles of orientation ang1, ang2, ang3 and ang4 for each layer of the laminate between 0^0 and 90^0, the thickness of the pressure vessel **t** will be between 0.0in and 1.5in, the status variable is associated with failure criterion FcMax or will be in the range [0.0 … 1.0] and that will be calculated by ANSYS.

In each iteration of the algorithm, performs a thickness variation **t** as well as angular rotation of the laminate sheets that are associated with the angles ang1,ang2,ang3,ang4; each *thread* receives by parameter the characteristics of different particles(information related to the thickness and angles) to be evaluated by FEM in ANSYS, who returns the failure rate, volume, offset , deformation and tension between other outputs; depending on the criterion of judgment, the process is repeated and generate new features to update to the particles of space solution that they return to be evaluated until the failure to first sheet (criterion of failure of Tsai-Wu) ending and leaving a series of feasible values recorded in a file, which will take the best of them.

Since the *threads* abstract criteria related to multiprocessing[34] as reflected in the *states of execution of a thread* (Fig. 3) and taking advantage of the concept of time share to save computing times[35], we use *threads* to interact with ANSYS in *batch mode* and since they run the script in APDL; the implementation of a single script to evaluate a particle at each iteration of the optimizer, consume a compute time **tc** that by the total number of **m** particles would give us a total time $tt = tc \cdot m$, which would affect the performance of the PSO; so that, when executed **n** threads in the same space of time **tc** would reduce approx. $\frac{1}{n}$ The total processing time of the **m** particles by what $tt = \frac{1}{n} \cdot tc \cdot m$; since with the threads can be used by those time intervals in which the central processing unit (CPU) is free, while other components are running part of the process, then you can compensate for times of computing with overlapping execution of threads in the same space of time and in this way we will compensate the runtimes of the PSO.

3.-RESULTS

Table 2 contains the result of the optimization, records the failure rate FcMax(criterion of Tsai-Wu), angle of the sheeting ang1,ang2,ang3,ang4, thickness of the pressure vessels t, optimized TVolume, volume displacement; are recorded results of 10 iterations, the first 9 are feasible and the last exceeds the failure rate established; the last column reflects the M5[21] before optimization.

Iterations		set 1	set 2	set 3	set 4	set 5	set 6	set 7	set 8	set 9	set 10	M5
Objective		(feasible)	(feasible)	(feasible)	(feasible)	(feasible)	(feasible)	(feasible)	(feasible)	(feasible)	(infeasible)	no optimized
FcMax(SV)	-	0.8697	0.8871	0.9018	0.9071	0.9721	0.9725	0.9793	0.9815	0.9945	1.0339	0.9040
ang1(DV)	°	73.49	81.41	81.11	76.61	81.62	83.64	82.10	83.64	83.64	76.34	45.00
ang2(DV)	°	31.98	18.06	24.67	27.40	14.83	5.86	9.99	5.86	5.86	22.80	45.00
ang3(DV)	°	46.72	25.45	38.09	39.44	21.37	10.20	18.93	10.20	10.20	38.00	0.00
ang4(DV)	°	71.47	73.99	74.37	73.97	75.36	85.71	75.52	85.71	85.71	73.62	90.00
t(DV)	in	1.0341	0.7458	0.8449	0.8854	0.6779	0.6200	0.6533	0.6166	0.6100	0.7672	0.7500
	mm	26.27	18.94	21.46	22.49	17.22	15.75	16.59	15.66	15.49	19.49	19.05
TVolume(OBJ)	in³	3133.83	2319.6	2604.56	2719.61	2121.17	1949.79	2048.4	1939.6	1920.19	2381.38	2331.91
	mm³	0.0514	0.0380	0.0427	0.0446	0.0348	0.0320	0.0336	0.0318	0.0315	0.0390	0.0382
weight of the toroid	Kg	82.11	60.77	68.24	71.25	55.57	51.08	53.67	50.82	50.31	62.39	61.10
displacement DMX	in	0.0307	0.0402	0.0356	0.0344	0.0453	0.0474	0.0482	0.0477	0.0507	0.0404	0.0440
	mm	0.78	1.02	0.90	0.87	1.15	1.20	1.22	1.21	1.29	1.03	1.12

Table 2: Results of the Optimization

In (Fig.4a) are shown the curves of design variables ang2 and ang3 have decreasing trends while ang1 and ang4 have increasing trends.

The (Figure 4c) shows that the volume of the toroidal pressure vessel wall is minimized at the same time that the thickness of the laminate is reduced (Figure 4b) which also affects the weight of the toroidal pressure vessel (Fig.4f) whose curve shows that this also decreases, the three curves reflect a similar behavior and their trends are decreasing; this reduction of volume, weight and thickness in the toroid to a constant pressure affect the same displacement that shows a rising trend (Fig.4e). On the other hand, the failure rate determines the optimization as a variable of state, his curve shows an increasing trend since this should reach 1 to finish the process.

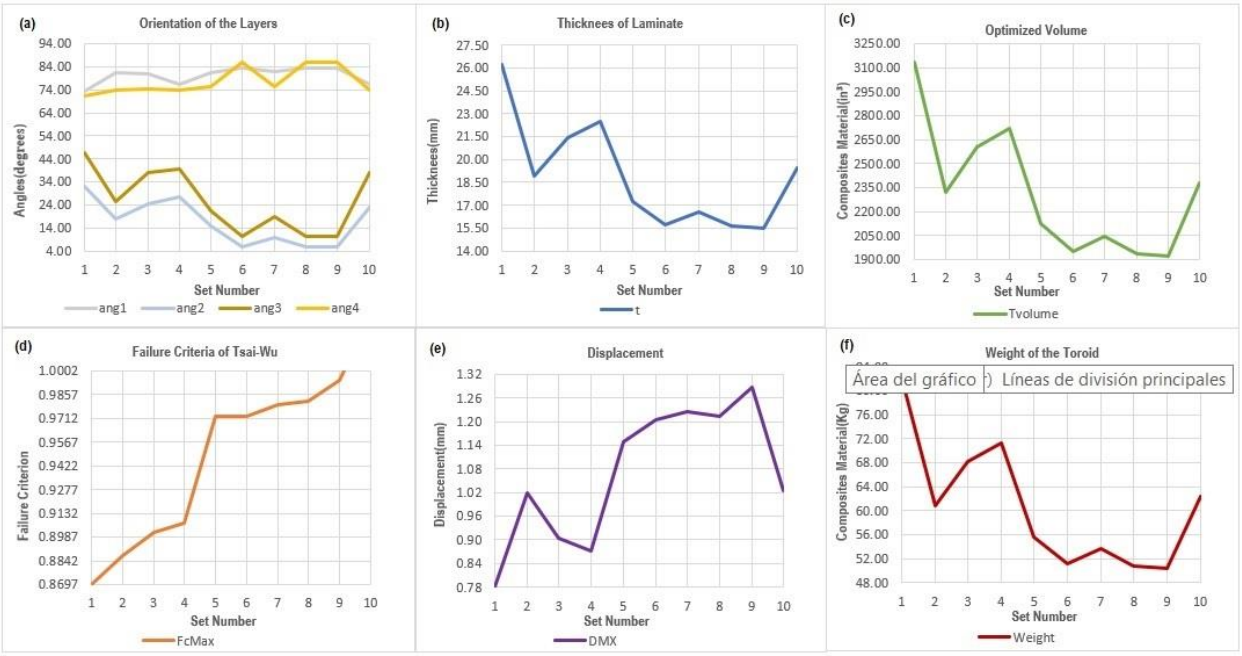

Fig. 4. Curves of the Optimization Results

With the data in the columns **set9** and with the last column in the Table 2, we generated the toroid models M5 and M6 not optimized toroid, have equal dimension, but differ by the thickness of the wall and the angles of orientation of the sheets of laminate flooring.

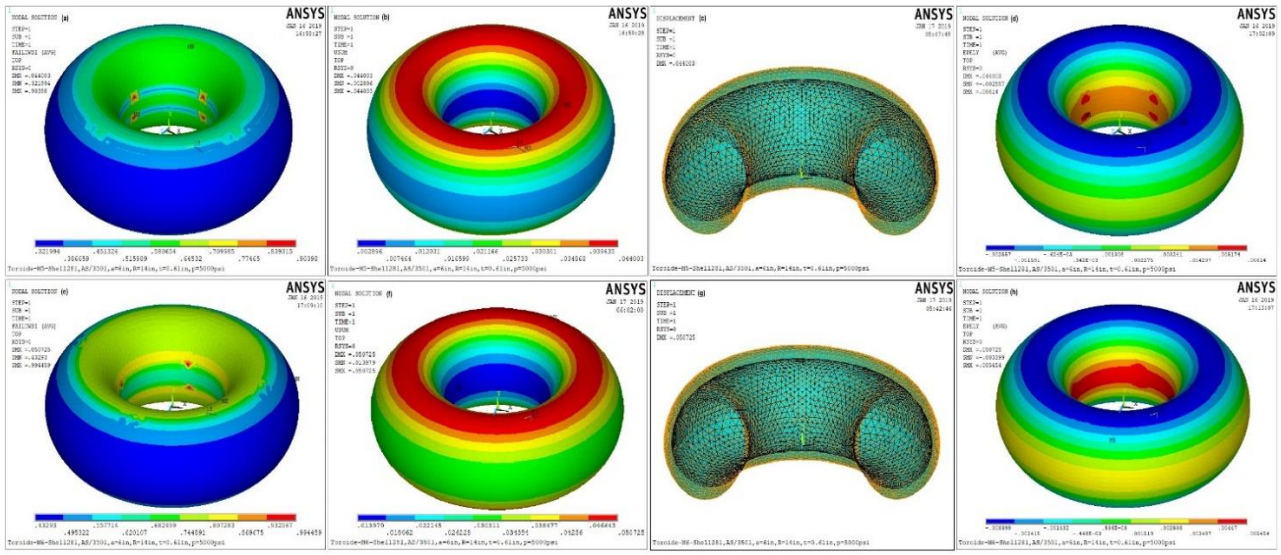

Fig. 4. Toroidal optimized model M6

The (Figure 4e) reflects that failure rate of M6(0.9945) has increased 10% compared to the rate of M5(0.90398) according to (Fig.4a), in both cases MX points out that the fault will occur on axial area of the toroid.

The (Figure 4b) reflects that the displacement of 0.0507M6(in) has increased by 15.23% with respect to M5(0.044in) according to (Figure 4f); in both cases MX points out that in the crest of the toroid is where further displacement; figures (Figure 4c and 4g) reflect a cross section of the toroid and it can be seen that the circumferential areas expand and axial areas are collapsed.

The (Fig. 4d) shows that the rate of deformation of M6(0.005454) has been reduced the 11.17% with respect to M5(0.00614) according to (Figure 4h), in both models causes deformations in the circumferential areas of the toroid, but with greater intensity in their areas axial.

4.- DISCUSSION AND CONCLUSIONS

The amount of the material M5(61.1Kg) to be optimized M6(50.3Kg) was reduced by 17.7%, causing a shift in the 15% although the deformation has decreased 8%, it should be noted that the volume of material has varied in the same percentages, so that the thickness t=0.61in (15.49mm) reduced the approx. 18.7% compared with initial model t=0.75in (19.05mm), therefore the variation of the angles of the layers of laminate have influenced the results obtained, maintaining the resistance of the laminate of the container at 5000psi (374.44bar) of pressure to which it was subjected.

Pressure Vessel	Weight of Material (Kg)	Pressure Sopported (psi)	Pressure Sopported (bar)	Capacity (L)	Weight of CNG (Kg)	Energy that can store (Kcal)
Toroid M5(noOPT)	61.1	5000	344.74	163.03	42.72	512212.8
Toroid M6(OPT)	50.3	5000	344.74	163.03	42.72	512212.8
Steel Cylinder[39]	80	2900.75	180	80	12.9	154671
Plastic Cylinder + Carbon Fiber Reiforcement [39]	34	2900.75	200	74	11.9	142681
Cylinder Type I [3]	194	2900.75	200	200	11.6	139084
Cilinder Type II [3]	70	2900.75	200	100	13.5	161865
Calorific Power of CNG	11990 Kcal/Kg					
Ideal Gas Ecuation	Pressure.Volume = number of moles.R(universal constant).Temperature					
	Number of Moles = mass / molecular mass					

Table 3: Comparative Analysis Cylindrical Pressure Vessels and CNG Toroidal Pressure Vessel

The Table 3 reflects four types of cylindrical pressure vessels[36] for the storage of CNG, peak pressures supported are approx. 200bar, with a margin of safety approx. 26.7%, these designs can contain up to 15Kg of CNG but the maximum permissible load is 11Kg. In the energy market[37] it is established that 1Kg of CNG=1.5L of gasoline=1.025L de gasoil; since the toroidal pressure vessels M6 can store 42.72Kg of CNG=64.08L de gasoline=43.79L de gasoil, in comparison with the cylinder type II that can store 13.5Kg of CNG=20.25L of gasoline=13.84L of gasoil, the M6 toroidal pressure vessels stores approx. 3 times more of what you can store the traditional cylinder.

The amount of CNG energy that can store M6 provides you with 512221.8Kcal of energy that is 3 times more than what you get with the cylinder type II (161865Kcal), so that the autonomy that can be achieved with a vehicle with these toroidal pressure vessels would be very beneficial.

The cylindrical pressure vessels have different dimensions to the toroidal pressure vessels, its geometric mean toroidal causes waste of space inside the trunk of the car; M6 has the dimensions of a tire by its shape provides a space savings in the compartment, the storage capacity is 163.03L equivalent to 42.72Kg of CNG that is times 208.4% more than what can be stored in the cylinder type II reflected in Table 3.

By what was analyzed, it was concluded that the toroidal pressure vessels optimized M6 offers very good performance for the storage of CNG, the manufacture of this type of pressure vessels with composite materials would provide a significant advance in this field by the economic benefits and energy that provides the CNG.

REFERENCES

[1] Khan, M.I., Yasmin, T., Shakoor, A.: Technical overview of compressed natural gas (CNG) as a transportation fuel. Renew. Sustain. Energy Rev. (2015). https://doi.org/10.1016/j.rser.2015.06.053
[2] Sirosh, N., Niedzwiecki, A.: Development of storage tanks: High-pressure vessels, http://www.scopus.com/inward/record.url?eid=2-s2.0-73749087443&partnerID=tZOtx3y1, (2008)
[3] COMPRESION, K.: Cilindros GNC Vehicular, http://www.kioshicompresion.com/vehicular.html
[4] Cook, J., Richards, B.J.: Aparato de Contención de Gas, (2002)
[5] Fowler, C.P., Orifici, A.C., Wang, C.H.: A review of toroidal composite pressure vessel optimisation and damage tolerant design for high pressure gaseous fuel storage. Int. J. Hydrogen Energy. 41, 22067–22089 (2016). https://doi.org/10.1016/j.ijhydene.2016.10.039
[6] Miravete, A.: Materiales Compuestos. Volumen I i II. Mater. compuestos. (2000). https://doi.org/10.3989/mc.2010.46908
[7] Park, S.J., Kim, B.J.: Carbon fibers and their composites. Springer Ser. Mater. Sci. (2015). https://doi.org/10.1007/978-94-017-9478-7_8
[8] Huang, X.: Fabrication and properties of carbon fibers, (2009). https://doi.org/10.3390/ma2042369
[9] Boeing: Recuperado de:www.boeing.com, www.boeing.com
[10] Airbus: Recuperado de:www.airbus.com, www.airbus.com
[11] Ferrari: Recuperado de www.ferrari.com, www.ferrari.com
[12] Maksimyuk, V.A., Chernyshenko, I.S.: Nonlinear elastic state of thin-walled toroidal shells made of orthotropic composites. Int. Appl. Mech. (1999). https://doi.org/10.1007/BF02682397
[13] Park, J.S., Hong, C.S., Kim, C.G., Kim, C.U.: Analysis of filament wound composite structures considering the change of winding angles through the thickness direction. Compos. Struct. (2002). https://doi.org/10.1016/S0263-8223(01)00137-4
[14] Zu, L., Koussios, S., Beukers, A.: Pattern design and optimization for filament - wound toroidal pressure vessels. In: 23rd Technical Conference of the American Society for Composites, Memphis, TN, USA (2008)
[15] Zu, L.: Stability of fiber trajectories for winding toroidal pressure vessels. Compos. Struct. (2012). https://doi.org/10.1016/j.compstruct.2011.11.027
[16] Hu, H., Li, S., Wang, J., Zu, L.: Structural design and experimental investigation on filament wound toroidal pressure vessels. Compos. Struct. (2015). https://doi.org/10.1016/j.compstruct.2014.11.023
[17] Yang, F., Wang, P., Zhang, Y., Zheng, L., Lu, J.: Survey of swarm intelligence optimization algorithms. In: Proceedings of 2017 IEEE International Conference on Unmanned Systems, ICUS 2017 (2018). https://doi.org/10.1109/ICUS.2017.8278405
[18] Kennedy, J., Eberhart, R.: Particle swarm optimization. Proc. ICNN'95 - Int. Conf. Neural Networks. (1995). https://doi.org/10.1109/ICNN.1995.488968
[19] Tao, W., Liu, Z., Zhu, P., Zhu, C., Chen, W.: Multi-scale design of three dimensional woven composite automobile fender using modified particle swarm optimization algorithm. Compos. Struct. (2017). https://doi.org/10.1016/j.compstruct.2017.08.065
[20] Poli, R., Kennedy, J., Blackwell, T.: Particle swarm optimization. Swarm Intell. (2007). https://doi.org/10.1007/s11721-007-0002-0
[21] Patiño, D., Corz, A.: Análisis Comparativo de Recipientes a Presión Toroidal de Material Compuesto por Elementos Finitos [Comparative Analysis of Toroidal Pressure Vessels of Composite by Finite Elements]. Int. J. Innov. Appl. Stud. 25, 162–175 (2018)
[22] Vick, M.J., Gramoll, K.: Finite Element Study on the Optimization of an Orthotropic Composite Toroidal Shell. J. Press. Vessel Technol. 134, 051201 (2012). https://doi.org/10.1115/1.4005873
[23] Li, S., Cook, J.: An Analysis of Filament Overwound Toroidal Pressure Vessels and Optimum Design of Such Structures. J. Press. Vessel Technol. 124, 215 (2002). https://doi.org/10.1115/1.1430671
[24] Herakovich, C.T.: Mechanics of Fibrous Composites. In: John Wiley and Sons. , New York (1998)
[25] Reddy, J.N.: Mechanics of Laminated Composite Plates and Shells: Theory and Analysis, Second Edition -. Book. (2003). https://doi.org/10.1038/sj.leu.2403242
[26] Tsai, S. W., Hahn, H.T.: Introduction to Composite Materials. , Westport (1980)
[27] Barbero, E.J.: Introduction to Composite Materials Design, Second Edition. (2010)
[28] Jesus, D., Gonzalez, J.: ScienceDirect Pressure based approach for Automated Fiber Placement (AFP) with sensor based Pressure based approach for Automated Fiber Placement (AFP) with sensor based Pressure based feedback approach loop for Automated Placement in the feedback loo. IFAC-PapersOnLine. 50, 794–799 (2017). https://doi.org/10.1016/j.ifacol.2017.08.511
[29] Contreras, A.J.: engineering & materials Ultimate breakthroughs in materials engineering Tecnología de laminado automatizado en materiales compuestos. 1–8 (2018)
[30] Springer, G.S., Kollar, L.P.: Displacements, Strains, and Stresses. In: Mechanics of composite structures (2003). https://doi.org/10.1016/0263-8223(94)90053-1
[31] Barbero, E.J., Shahbazi, M.: Determination of material properties for ANSYS progressive damage analysis of laminated composites. Compos. Struct. (2017). https://doi.org/10.1016/j.compstruct.2017.05.074
[32] Chen, J., Tang, Y., Ge, R., An, Q., Guo, X.: Reliability design optimization of composite structures based on PSO together with FEA. Chinese J. Aeronaut. (2013). https://doi.org/10.1016/j.cja.2013.02.011
[33] Lili Liu, Shengxiang Yang, Dingwei Wang: Particle Swarm Optimization With Composite Particles in Dynamic Environments. IEEE Trans. Syst. Man, Cybern. Part B. 40, 1634–1648 (2010). https://doi.org/10.1109/TSMCB.2010.2043527
[34] Arora, N.S., Blumofe, R.D., Plaxton, C.G.: Thread scheduling for multiprogrammed multiprocessors. Theory Comput. Syst. (2001). https://doi.org/10.1007/s002240011004
[35] Threads, J.: Java threads. Comput. Math. with Appl. (1997). https://doi.org/10.1016/S0898-1221(97)84610-X
[36] Shijiazhuang Yunhong Trade Co., L.: recuperado: Cilindros De Gnc Para Vehículos,

https://cnyunhong.en.alibaba.com/company_profile.html
[37] Lage, M., General, S.: El gas natural en la movilidad La alternativa renovable. 1–16 (2017)